OLTARIS: On-Line Tool for the Assessment of Radiation In Space

Robert C. Singleterry Jr., Steve R. Blattnig, Martha S. Clowdsley,
Garry D. Qualls, Chris A. Sandridge, Lisa C. Simonsen, John W. Norbury
NASA Langley Research Center, Hampton, Virginia
Tony C. Slaba, Steve A. Walker
Old Dominion University, Norfolk, Virginia
Francis F. Badavi
Christopher Newport University, Newport News, Virginia
Jan L. Spangler
Lockheed Martin Operations Support, Hampton, Virginia
Aric R. Aumann
Analytical Services and Materials, Hampton, Virginia
E. Neal Zapp, Robert D. Rutledge, Kerry T. Lee
Johnson Space Center, Houston, Texas
Ryan B. Norman
University of Tennessee, Knoxville, Tennessee

The On-Line Tool for the Assessment of Radiation In Space (OLTARIS) is a World Wide Web based tool that assesses the effects of space radiation to humans in items such as spacecraft, habitats, rovers, and spacesuits. This document explains the basis behind the interface and framework used to input the data, perform the assessment, and output the results to the user as well as the physics, engineering, and computer science used to develop OLTARIS. The physics is based on the HZETRN2005 and NUCFRG2 research codes. The OLTARIS website is the successor to the SIREST website from the early 2000's. Modifications have been made to the code to enable easy maintenance, additions, and configuration management along with a more modern web interface. Over all, the code has been verified, tested, and modified to enable faster and more accurate assessments. The next major areas of modification are more accurate transport algorithms, better uncertainty estimates, and electronic response functions. Improvements in the existing algorithms and data occur continuously and are logged in the change log section of the website.

I. Introduction and Background

Particle transport algorithms and methods needed to assess the radiation shielding in spacecraft are difficult to solve and master. When non-experts are asked to utilize them in their normal work flow, the functionality of these algorithms and methods needs to be simple, clear, and straight forward. The answers that they give need to be accurate, characterized by an uncertainty, and reproducible.[1,2] Achieving these goals entails numerous characteristics: modularity, version control, modern user interface, maintainability, verification, and validation. Data interfaces and formats need to be established between modules, clear paths need to be established for data flow, and user interfaces need to feed the proper data into and out of the system so that a non-expert user can understand the input and results.

A first attempt at this type of functionality for space radiation was achieved with the SIREST website.[3] OLTARIS is its successor, as the problems SIREST faced to meet modeling and simulation requirements were overwhelming.

The first task was to establish acceptable user interactions with the website. This was achieved through interviewing potential users about how they envisioned working with this type of data. Use cases were gener-

ated to capture this desired work flow and functionality. From these initial use cases and other programmatic requirements, an initial capability was defined.

Current, state-of-the-art, research-based radiation analysis tools were identified and utilized in the construction of OLTARIS. The research-based particle radiation transport code HZETRN2005[4,5] is the basis for OLTARIS. HZETRN2005 has embedded response functions that were greatly expanded in OLTARIS. New response functions not in HZETRN2005 were also added. The NUCFRG2[6–8] code was used for heavy ion cross sections with HZETRN2005 embedded light ion cross sections.[9]

As OLTARIS becomes more robust and able to solve a broader range of space radiation problems, its applicability to other space design, simulation, and operations communities grows. Therefore, it is incumbent upon the developer group to introduce it to a broader range of potential users.

The rest of the paper will describe in detail the current capability and how that capability was implemented on OLTARIS.

II. OLTARIS Description and Functionality

The OLTARIS architecture is divided into two main parts, the website, in which users interact through a browser, and the execution environment, where the computations are performed. This architecture enables maximum flexibility and is scalable as demand increases. The website is built primarily with standard open source components. The core is Ruby on Rails[10] with a MySQL[11] database running on an Apache[12] web server. The only licensed, server-side component is an Adobe Flash plugin which allows the users to plot and examine results using a standard, free plugin that most browsers already have.

The execution environment is primarily FORTRAN executables tied together with some Perl and Ruby scripts running on a computational cluster. Data is passed between the web server and the cluster using XML files. Jobs are managed with the open-source Sun Grid Engine (SGE).[13] There are benefits to having SGE serve as a mediator between the user interface and the computations. First, additional nodes or clusters can be easily added as demand increases. Also, we can easily replace the web interface with a desktop client sometime in the future, if requirements dictate.

Figure 1 shows the program and data flow for OLTARIS. The boxes indicate different components or modules of the system. This modular system makes it easy to maintain and upgrade as new algorithms, methods, and capabilities are developed. Each module has a clearly defined input and output data format so that the individual module developers don't have to know about the details of the other modules. For example, if requirements dictate the development of another radiation environment, the new radiation environment will plug in to the process cleanly, as long as its outputs are in the same format as every other environment model.

The green boxes indicate the data that the user needs to supply: a slab definition or a thickness distribution of their vehicle (see Section II.B), and mission parameters that will determine how the external radiation environment is computed. The blue boxes indicate data that the user can either download from the web server or data used in the calculations and stored on the execution host. This includes material data with associated cross section databases (see Section III) and body-thickness distributions used in the calculation of whole-body effective dose equivalent. The downloadable content includes ray distributions and a phantom human CAD (Computer Aided Design) object that can be used to prepare the vehicle thickness distributions. The gold boxes represent the computations which are performed on the execution host and consist of three modules: the environmental model, the particle transport, and the response functions.

The environment module is where the external radiation environment is computed. The user can currently choose from three different types of environments: an historic Solar Particle Event (SPE) or a linear combination of events, free-space Galactic Cosmic Rays (GCR), or Low Earth Orbit (LEO). The output of these environments is a spectral flux or fluence (in units of $\frac{particles}{cm^2-AMeV-time}$, where time is given in events for SPE - fluence and days for GCR and LEO - flux). This flux/fluence is then used as the boundary condition for the transport. More details about the environments can be found in Section IV.

The transport module is composed of two paths depending on the type of geometry the user selects, either slab or thickness distribution. Both paths use nuclear transport methods based on HZETRN2005, which have been greatly improved, verified, and validated. The slab computation transports particles from the chosen boundary condition, through user defined materials, to generate fluxes/fluences at the material interfaces and at the end boundary. The computation for the case of a thickness distribution is a series of transport runs for an array of depths for each material that the user needs. OLTARIS currently supports aluminum,

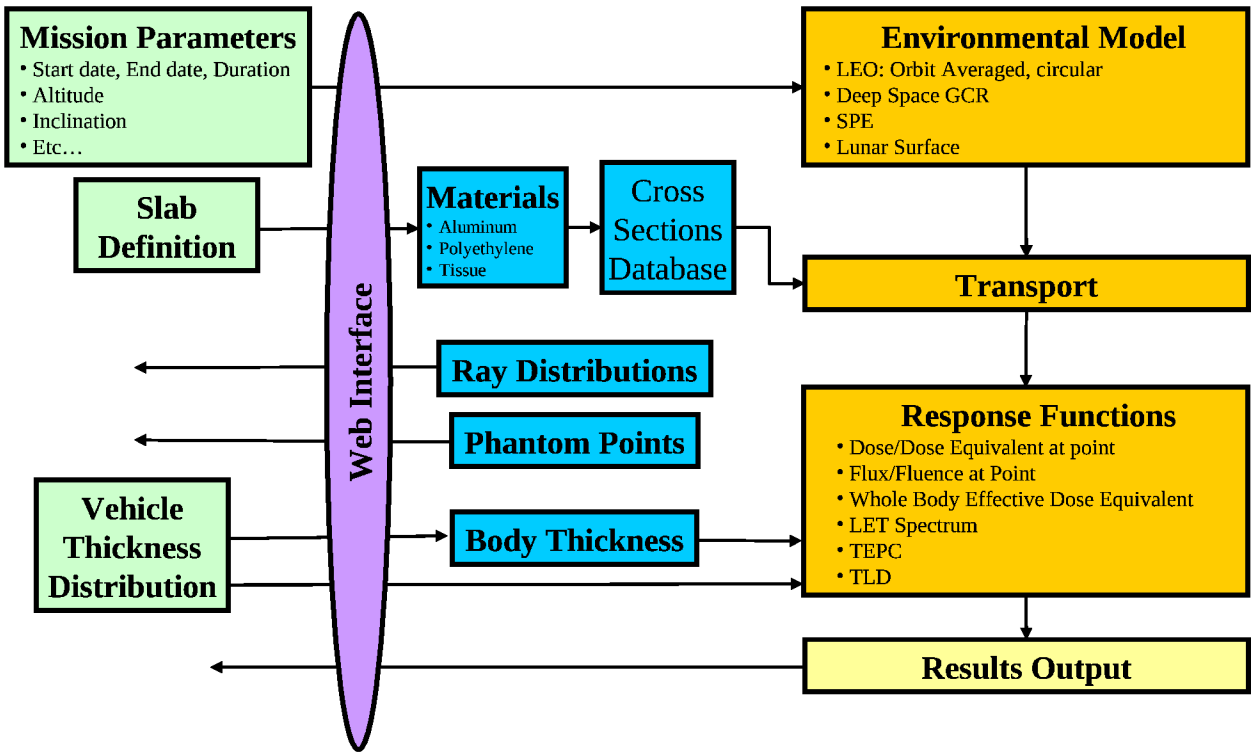

Figure 1. Program Flow for OLTARIS

polyethylene, and tissue for vehicle thicknesses. The output is an array of flux/fluence versus energy and thickness for every combination of material thicknesses. The selection of the spatial grid (thickness intervals) and the energy grid is dependent on the boundary condition and is not user selectable at this time. Further details about the transport method can be found in Section V.

The response function module takes the resulting flux/fluence calculated with the transport module and computes selected responses for each depth of the various materials and the total responses at the end of the slab or at the selected vehicle location. For thickness distributions, an array of response function versus depth curves are computed for the same set of material spatial grids selected for the flux/fluence transport. Total quantities along each ray in the thickness distribution are calculated by interpolating over the response function versus depth database just computed, and then integrating over all of the rays. In the case of whole body effective dose equivalent (or *effective dose*), an added step is performed to combine the vehicle thicknesses with the body thicknesses at the organ points for the Computerized Anatomical Female (CAF),[14,15] Computerized Anatomical Man (CAM),[16] Male Adult voXel model (MAX),[17] and Female Adult voXel model (FAX).[18] Details about all the possible responses can be found in Section VI.

Finally, all the results are transferred back to the user's account on the website for viewing, plotting, or download.

A. Web interface

Users need to register on OLTARIS and get approval before they can enter the website. This is required because some of the content falls under the purview of the International Traffic in Arms Regulations (ITAR),[19] but it also allows for regulating and maintaining limited computer resources by permitting only those with a real need and knowledge to access the site. Once the user account has been activated by a site administrator, the user can login and start using the tools.

The first page the user sees after login is the *Projects* page. Each project is the complete encapsulation of a calculation; it includes the definition of the radiation environment, the selection of a thickness distribution or slab, and a selection of desired responses. This page allows the user to create new projects, edit existing

projects, submit new jobs to the compute cluster, and access the results of previous jobs. A job is an instantiation of a project that is packaged for processing. When a new project is created, the user is stepped through a series of pages that allows them to define the different aspects of the problem. Help pages are available at any point in the process if the user needs more information. Once the project is saved, the user is returned to the *Projects* page and can submit a job to the compute cluster. A project can include multiple jobs so that if the user wants to change particular elements of the project, say select a different environment or response, the user can do so and create an additional job that can be submitted under that same project.

Once a job is submitted, the user can check on the status of the job from the *Jobs* page for the project. Also, when a job is complete, an email will be sent to the user from the grid scheduler (SGE). Once the job is complete, the user can view the results by selecting *Display/Download Results* for the completed job on the *Jobs* page. The results page will list some of the results directly in tabular form and allow the user to plot data such as dose versus depth curves and flux/fluence data. The plot page has the option to copy the plotted data to the user's clipboard so that it can then be pasted into various local applications on their computer. The user also has the option to download the data to their desktop computer in the form of an ASCII compatible file.

Another section of the website is the *Thickness Distributions* page which is selected from one of the main tabs across the top of the page. This page presents a list of the user's current thickness distributions and allows the user to upload new ones. Once a thickness distribution is uploaded to the site, it is available for selection from a project page. Thickness distributions are uploaded to the site in the form of an XML file. A document describing the format of the file and sample files can be downloaded from the *Thickness Distributions* page. The user can also download a phantom CAD object that represents a human geometry. This can be positioned and oriented in the user's CAD software to help select the proper target points in their vehicle geometry and compute effective dose responses. The next section of this paper describes this process in more detail.

The *Slabs* and *Materials* sections, selected from the tabs at the top of each page, are used to create user-defined slabs of any material the user desires. The user first defines the materials they want to use at the *Materials* tab by entering the material's elemental mass percentage, its molecular mass percentage, or its chemical formula. Once the material is defined, the user can submit the material definition to the computational grid so that the material cross sections (see Section III) can be computed for later use. Once the cross section database is available, the user can then go to the *Slabs* tab and define a layup of any thickness of material, in any order they choose. This capability is useful for comparing new material or structural concepts. Once a slab is created, it can be selected for a project from the *Projects* page.

B. Thickness Distributions

In order to compute a response in a realistic vehicle geometry, a representation of the vehicle geometry, in the form of a material thickness distribution, is required. This thickness distribution is computed using a process called ray tracing. Ray tracing uses a directionally distributed set of rays emanating from the same point to determine how much material is surrounding that point in each ray direction. The point source of the rays is commonly called a Target Point. The intersections of the rays and the various components of the vehicle CAD model are used to determine the along-ray thicknesses of the components, which are stored along with their associated material types.

OLTARIS currently supports only three materials - aluminum, polyethylene, and human tissue, as mentioned previously. For example, one ray could intersect a human being, which would be a thickness of tissue, followed by some shielding material, which could be polyethylene, and then the vehicle structural components, which could be a thickness of aluminum. Rays typically intersect multiple objects, so there can be many separate material thicknesses along each ray. The current version of OLTARIS will sort and combine these thicknesses so that the outermost layer of shielding is composed of all the collected aluminum thicknesses along that ray, the next layer of shielding represents the total thickness of polyethylene along that ray and the innermost layer represents the total amount of tissue along that ray.

Any angular distribution of rays may be used, as long as they are distributed evenly enough that each ray can be considered to represent an equal solid angle of shielding surrounding its target point. However, to compute an effective whole-body dose equivalent using OLTARIS, the user will need to use one of the many ray distributions that are available for download from the Thickness Distributions page. Those currently available include distributions with 42, 492, 512, 968, 1002, 4002, 9002, or 10,000 rays. If the user needs to

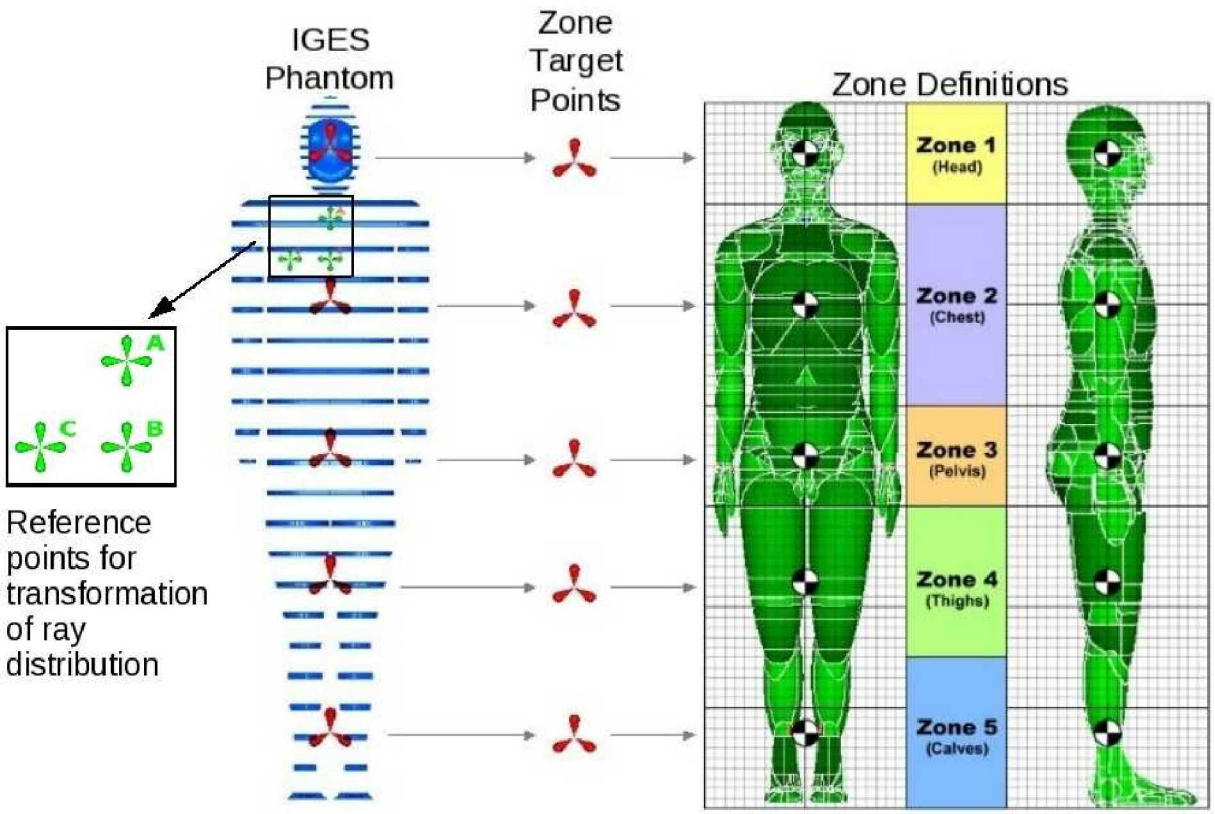

Figure 2. Body Phantom Zone Points

take into account a specific body phantom orientation with respect to their vehicle, OLTARIS provides a process that makes this possible.

To calculate an effective dose, OLTARIS combines uploaded vehicle thickness distributions with pre-computed body phantom thickness distributions. The process used to combine these distributions provides the ability to analyze a specific body orientation relative to a vehicle shielding model and the ability to capture the local variation of radiation intensity inside the vehicle. This local variation could be due to variations in the amount of shielding surrounding different regions of the vehicle interior and might, for example, yield a situation in which the phantom's head was more lightly shielded than its feet.

In order to accurately represent the user's desired phantom orientation within a vehicle model, the user will need to download one of two specially developed CAD models from the OLTARIS web site. These CAD models are proxies for the male and female body phantoms that are available for use in OLTARIS. The user will need to load this model into their CAD software, as a new component in their shielding model. The models have been made available in an IGES file format to gain broad compatibility with the widest possible array of CAD software. Each body phantom proxy CAD model includes eight reference points.

The three points used to establish the phantom orientation have been colored green and labeled "A", "B", and "C" (see Figure 2). Once oriented, the user will record the (x,y,z) coordinates of these three points, taking care to use the same reference coordinate system that will be used for ray tracing. The coordinates of these three points can be entered into a form on the OLTARIS website to generate a custom ray distribution, rotated to take the phantom orientation into account. The form used to create these ray distributions can be accessed from the *Thickness Distributions* page. The user should use this ray distribution to ray trace vehicle thickness distributions that correspond to that phantom orientation.

The other five reference points included with each IGES phantom proxy are colored red and are used to capture the effects of shielding variation within the vehicle interior. These five points correspond to five body zones, as shown in Figure 2. To use this feature, the user will need to perform five separate vehicle

ray traces and calculate five separate vehicle thickness distributions, each centered on one of the red zone target points. The effective whole-body dose equivalent calculation (See Section VI.E) within OLTARIS uses tissue thickness distributions based upon hundreds of target points that are distributed throughout the body phantom in specific tissues. OLTARIS will add the vehicle thickness distribution closest to each of the zone's tissue thickness distributions to get the total shielding around each body point. The user does not have to use the five target points, as one target point can be used in which all of the body points are added to the single vehicle thickness distribution. However, a single target point will be less accurate than the five target point case, as the local variations in the vehicle shielding may be significant.

C. Verification

Users expect to get reliable and accurate results from the tools that they use; therefore, OLTARIS has implemented several levels of verification to ensure consistent and accurate results. The OLTARIS system consists of thousands of lines of code, hundreds of files, and megabytes of data. All of the source code and data are stored in a version-control repository that all of the developers can access. This way, all changes are tracked and everyone can have access to the same code base. The source repository is organized along the lines of Figure 1 and each box has a specific developer who is responsible for, or *owns,* that module. Before any new methods or techniques are stored in the repository, the developer must ensure the accuracy of the method and write corresponding test cases that are also entered into the repository. These test cases are referred to as *module tests.* Test cases are also developed that test the interaction between modules or complete runs through the system; these are called *functional tests.* The combination of module and functional tests are intended to verify that the code base and data are generating consistent results. This suite of tests is automatically re-run periodically to make sure that any changes entered into the repository do not break the system somewhere else. If a discrepancy is found, the responsible developer is notified so they can fix the problem. Once the code has been sufficiently tested and is ready to be deployed, it is *tagged* or labeled for reference. This tagged version is a snapshot of the code base and is also noted at the bottom of every page on OLTARIS.

Verification through the web is not as automated as with the FORTRAN modules. The web code is maintained under version control, but the testing is manual. There is both a test website and a production website. The test site has its own server, database, and execution environment on the compute cluster, but it is only used by the developers. Projects can be set up and run on the test website and compared to runs made behind the scenes without the web code. Several developers test different paths in order to be sure everything is working properly. Once everything is working properly on the test system, the codes are deployed to the production site. There is also a *change log* on OLTARIS so that users can see when changes and updates are made that may change their results.

III. Material Properties

Material properties are an important part of the HZETRN2005 transport algorithm. Material dependent cross sections are used to predict the ways in which neutrons and charged ions will interact with shielding material. For vehicle thickness distributions, three materials (currently aluminum, polyethylene, and tissue) are used and their cross sections are pre-calculated. For slab based calculations, the user can input materials in numerous ways. These materials are then available for use in a pull-down list when defining slabs.

A material cross section is the probability of interaction between a particle projectile and the target nucleus with a particular outcome of that interaction. This probability is represented as the effective cross sectional area of the target nucleus as a function of the projectile energy and particle type. The unit is cm^2 and is usually represented as a *barn* or $10^{-24}cm^2$. An example of an interaction would be:

$$Fe^{56} + Al^{27} \longrightarrow C^{12} + X_Z^A$$

where Fe^{56} is the projectile, Al^{27} is the target, and X are the left over projectile and target fragments. The mass number, A, and the atomic number, Z, must add up to 71 and 33, respectively.

A. Heavy Ion Based Nuclear Cross Sections

It is important for OLTARIS to contain an analysis path that runs quickly and is fairly accurate. For transport algorithms, HZETRN2005, with NUCFRG2, satisfies this criterion. Monte Carlo codes, such as

FLUKA,[20] MCNPX,[21] GEANT,[22] PHITS,[23] HETC,[24] and MARS[25] may require shorter or longer running times in comparison to OLTARIS depending on the geometry input and the response wanted. In order to decrease the run time of nuclear physics codes, an interpolation scheme is used instead of running the codes for every interaction. Nevertheless, NUCFRG2 is able to run faster than nuclear physics models embedded in Monte Carlo simulations.

NUCFRG2 is a classical, geometric model based on the abrasion - ablation concept,[26] whereby a piece of the incoming projectile nucleus is sheared off (abraded) by collision with the target. The abraded piece is formed in a highly excited state, which subsequently decays (ablates) by energetic particle emission. The model is geometric in the sense that the entire abrasion - ablation process is determined by considering the relative impact parameter of colliding spherical nuclei. NUCFRG2 neglects quantum mechanical effects and does not include important shell structure information. Therefore, its most serious weakness is the inability to account for the odd - even effect observed in experimental data, where cross sections for fragments with an even number of nucleons are systematically larger than cross sections for fragments with an odd number of nucleons. This phenomenon is clearly related to the nuclear pairing interaction. Efforts are currently underway[27] to upgrade NUCFRG2 to include this effect, as well as to describe light ion production via coalescence.

B. Nucleon and Light Ion Based Nuclear Cross Sections

Total and differential energy cross sections for nucleon and light ion projectiles are handled outside of the NUCFRG2 model by a set of subroutines within OLTARIS. Processes relevant to the nuclear interactions of nucleons and light ions are utilized and include elastic scattering, light ion knockout and pickup, light ion projectile fragmentation, and target fragmentation. The cross sections for these processes are largely modeled by empirical and semi-empirical parameterizations.[4,9,28–34]

C. Atomic Based Cross Sections or Stopping Powers

The HZETRN2005 core routines solves the Boltzmann equation using the continuous slowing down approximation (CDSA) with stopping powers and residual ranges calculated using Bethe theory with corrections.[4,35] The transport solution uses scaled proton stopping power and ranges for all ions but directly calculates stopping power individually for each isotope when calculating some response functions.

IV. Radiation Environment or Boundary Conditions

The radiation environments within OLTARIS are computed in a modular fashion, whereby for a given spacecraft flight condition, the input particle(s) spectrum on the external boundary of the spacecraft has to be defined to initiate the transport through bulk matter. The input boundaries can be Galactic Cosmic Rays (GCR),[36,37] Solar Particle Events (SPE),[4,38–41] trapped proton/electron within the Earth's geomagnetic field,[42,43] and albedo neutrons from the Earth's atmosphere.[44–46] An energy spectrum for the particle field(s) with individual or combinations of these spectra, following a pre-determined I/O format to make them compatible with the transport as described in Section V, is generated. The following sections describe the possible boundary conditions.

A. Solar Particle Event Spectra

A solar particle event (SPE) is a large number of protons accelerated by the sun's magnetic fields towards a target, Earth in this case. The historical SPE events and their corresponding explicit differential formulas used in OLTARIS include[a]:

February 1956 Webber, with 100 MV rigidity:[38]

$$\phi(E) = 1.0 \times 10^7 \left[\frac{E+m}{\sqrt{E(E+2m)}} \right] \exp \left[\frac{239.1 - \sqrt{E(E+2m)}}{100} \right]$$

[a] m is the mass of the proton and is approximately 938 MeV

February 1956 LaRC:[4]

$$\phi(E) = 6.0 \times 10^7 \exp\left(\frac{10-E}{25}\right) + 9.375 \times 10^5 \exp\left(\frac{100-E}{320}\right)$$

November 1960:[4]

$$\phi(E) = 6.33 \times 10^8 \exp\left(\frac{10-E}{12}\right) + 4.88 \times 10^6 \exp\left(\frac{100-E}{80}\right)$$

August 1972 King:[39]

$$\phi(E) = 2.98 \times 10^8 \exp\left(\frac{30-E}{26.5}\right)$$

August 1972 LaRC:[4]

$$\phi(E) = 2.2 \times 10^7 \exp\left(\frac{100-E}{30}\right)$$

September 1989:[40] [b]

$$\phi(E \leq 10\text{MeV}) = 1.446 \times 10^8 \frac{E+m}{\sqrt{E(E+2m)}} \exp\left[\frac{-\sqrt{E(E+2m)}}{102.118}\right]$$

$$\phi(10\text{MeV} < E < 30\text{MeV}) = \left[-0.0015E^2 + 0.07184E + 0.4304\right]\phi(E \leq 10\text{MeV})$$

$$\phi(E \geq 30\text{MeV}) = \frac{2.034 \times 10^7}{\sqrt{1-\left(\frac{m}{E+m}\right)^2}}\left[\sqrt{\frac{E(E+2m)}{30(30+2m)}}\right]^{-4.5}$$

October 1989:[40]

$$\phi(E) = 6.104 \times 10^8 \left[\frac{E+m}{\sqrt{E(E+2m)}}\right] \exp\left[\frac{-\sqrt{E(E+2m)}}{92.469}\right]$$

Carrington 1859, with 1989 fit:[41]

$$\phi(E) = 0.877 \times 0.3841E^{0.3841-1} \times 4.79 \times 10^{11} \exp\left(-0.877E^{0.3841}\right)$$

Carrington 1859, with 1991 fit:[41]

$$\phi(E) = 0.972 \times 0.441E^{0.441-1} \times 1.47 \times 10^{12} \exp\left(-0.972E^{0.441}\right)$$

The boundary condition defines the units used in the rest of the OLTARIS processes. The units for all of the differential SPE spectra defined above are $\frac{protons}{cm^2-AMeV-event}$.

[b] A smoothing functions has been added in the 10 to 30 MeV range and $\phi(E \leq 10\text{MeV})$ in the smoothed equation is evaluated at the input energy range between 10 MeV and 30 MeV

B. Galactic Cosmic Rays

The model developed by O'Neill[36] is used as GCR input for OLTARIS. This GCR model is based on fitting the existing balloon and satellite measured energy spectra from 1954 to 1992 with more recent measurements from the Advanced Composition Explorer (ACE) satellite from 1997 to 2002 with the stationary Fokker-Planck equation. This fit solves the diffusion, convection, and energy loss boundary value problem and obtains an estimate of the appropriate diffusion coefficient. In addition, correlation of the diffusion coefficient with the Climax neutron monitor data, which exhibits an odd-even cycle with a 22 year period, enables the estimation of the diffusion coefficient at times when direct observational data are not available. The implementation of this GCR model accurately accounts for the solar modulation of hydrogen through nickel by propagating the Local Interplanetary Spectrum (LIS) of each element through the heliosphere. The model provides a single value of the deceleration parameter $\phi(t)$ describing the level of solar cycle modulation and determines the GCR differential energy spectrum for elements hydrogen to nickel at any given radial distance from the sun.

The earliest date available for input into the system is 01-Jan-1951. The latest date is variable and is controlled by the OLTARIS user interface. Please check the website for the latest date available. The user has three input methods:

1. Start and end dates from pull-down lists of the day, month, and year.
2. Start date from pull-down lists of the day, month, and year and the mission duration in days.
3. Preset scenarios with mission duration in days.

There are currently eleven preset scenarios available for user selections. Table 1 outlines the deceleration parameter for each of the scenarios. The boundary condition defines the units used in the rest of the OLTARIS processes. The units for GCR defined above are $\frac{particles}{cm^2-AMeV-day}$.

Table 1. Deceleration Parameters for Preset OLTARIS GCR Scenarios

Scenario	Deceleration Parameter
1956 Solar Min	401
1959 Solar Max	1986
1965 Solar Min	510
1970 Solar Max	1293
1977 Solar Min (DSNE[c])	474
1982 Solar Max	1924
1987 Solar Min	467
1991 Solar Max	2525
1997 Solar Min	467
2000 Solar Max	1674
2007 Solar Min (predicted)	490

[c]DSNE - Constellation Program Design Specification for Natural Environments[37]

C. Low Earth Orbit

The LEO boundary condition consists of three components: GCR, omni-directional trapped protons and electrons, and atmospheric albedo neutrons. Currently, OLTARIS does not transport the electrons and their flux is not accessible from the interface.

There are several options for specifying a LEO environment on OLTARIS. The user can input mission dates with altitude and inclination or select the DSNE environment (Constellation Program Design Specification for Natural Environments[37]), which will fix the dates, altitude, and inclination. The user can also select which of the three components are to be included.

1. Galactic Cosmic Rays

The GCR model of Section IV.B is modulated by a direction averaged geomagnetic transmission coefficient scaled by global vertical cutoff data using the model in references[47–49] to produce charge and energy dependent differential spectra. The acceptable altitude range for input is 200 to 20,000 km. The units of this boundary condition are in $\frac{particles}{cm^2-AMeV-day}$.

2. Omni-directional Trapped Protons and Electrons

The trapped proton model is calculated using AP8MIN and AP8MAX proton flux models based on the Vette reduction of satellite data.[42,43] AP8MIN is interpolated on the Jenson and Cain[50] geomagnetic field model and AP8MAX is interpolated on the Cain[51] geomagnetic field model extrapolated forward in time to 1970. As a side note, within the South Atlantic Anomaly (SAA) region, the trapped proton field dips down to about 200 km, which is well within the orbits of the STS and ISS missions. The acceptable altitude range for input is 200 to 20,000 km. The units of the omni-directional trapped proton and electron flux are $\frac{particles}{cm^2-AMeV-day}$.

3. Atmospheric Albedo Neutrons

Atmospheric albedo neutrons result from the interaction of GCR with the Earth's atmosphere. As the GCR intensities are modulated by solar activity so are the atmospheric neutrons modulated with time. The atmospheric neutron model[45] is a parametric fit to data gathered by NASA Langley Research Center's studies of the radiations at Supersonic Transport altitudes in the years 1965 to 1971. It covers the rise and decline of solar cycle 20. Scaling of the data with respect to geomagnetic cutoff, altitude, and modulation of the Deep River Neutron Monitor (DRNM) was found to allow for mapping of the environment to all locations at all times. This results in an empirically based model for the atmospheric albedo neutrons used in OLTARIS. The units of the atmospheric albedo neutrons flux are $\frac{neutrons}{cm^2-AMeV-day}$.

D. Lunar Surface

The lunar surface environment is currently implemented on OLTARIS in a simplified manner. The user can select either a lunar SPE or a lunar GCR environment. In each case, the corresponding free-space spectrum is computed and then applied to all of the rays in the vehicle thickness distribution not pointing toward the lunar surface. The surface pointing rays, which must be indicated in the thickness distribution, will have a *zero* boundary applied, which is an approximation since there is a neutron albedo spectrum coming from the surface. At this time, a lunar neutron albedo spectrum has not been implemented, so this zero-contribution from the surface is an approximation. The lunar albedo will be added as a future enhancement to OLTARIS.

V. Particle Transport

The particle transport module in OLTARIS currently uses HZETRN2005 core routines with NUCFRG2 as the heavy ion interaction cross sections and the HZETRN2005 embedded light ion cross sections. It is used to propagate particles of an ambient space radiation environment (See Section IV) through a combination of vehicle, shielding, and/or tissue. HZETRN2005 and NUCFRG2 were developed by Wilson et al.[4,9,52] and Cucinotta[53] with recent modifications and improvements provided by Slaba et al.[54] The HZETRN2005 transport algorithms provide approximate numerical solutions to the linearized Boltzmann transport equation with the Continuous Slowing Down Approximation (CSDA) and the straight ahead approximation[4] to yield:

$$\left[\frac{\partial}{\partial x} - \frac{1}{A_j}\frac{\partial}{\partial E}S_j(E) + \sigma_j(E)\right]\phi_j(x,E) = \sum_k \int_E^\infty \mathrm{d}E'\ \sigma_{k\to j}(E'\to E)\phi_k(x,E') \tag{1}$$

with the boundary condition

$$\phi_j(0,E) \ = \ f_j(E),$$

where $\phi_j(x,E)$ is the flux or fluence of type j particles at depth x with kinetic energy E. In equation 1, A_j is the atomic mass number of a type j particle, $S_j(E)$ is the stopping power of a type j ion with kinetic energy E, $\sigma_j(E)$ is the total macroscopic cross section for a type j particle with kinetic energy E, and

$\sigma_{k\to j}(E' \to E)$ is the macroscopic production cross section for interactions in which a type k particle with kinetic energy E' produce a type j particle with kinetic energy E. The summation limits in equation 1 will be discussed shortly. The boundary condition spectrum, $f_j(E)$, is considered to be a known function over a broad energy spectrum and has been discussed in Section IV.

The left hand side is known as the Boltzmann operator, and the right hand side is the scattering kernel or collision operator. The Boltzmann operator in equation 1 consists of a streaming term in one dimension of space and no dimensions of angle, the CSDA term in energy, and the total interaction probability. The scattering kernel sums and integrates over all particles and energies to represent the source of secondary particles produced through fragmentation and elastic interactions.

The CSDA is based on the assumption that sufficiently many atomic interactions occur per unit path length to allow them to be expressed as a continuous process. The straight ahead approximation is based on the assumption that all primary and secondary particles propagate in the same direction and reduces the transport equation to one spatial dimension and no angular dimensions. The particle source is the boundary condition; therefore, a marching algorithm can be used to solve the equations in the direction of interest.

Transport solutions for light ions (A≤4) (including neutrons) and heavy ions (A>4) are obtained separately as demanded by the treatment of the nuclear cross sections and external space radiation environments. For heavy ions, it is known that prompt projectile fragments have a velocity, or energy per mass unit, very near that of the projectile (the constant velocity approximation), while de-excitation particles from the projectile fragments are produced nearly isotropically with lower energy.[5] The heavy ion projectile's target nuclei's fragments are neglected in the transport procedure due to their low energy and hence range. These approximations greatly simplify the transport equation (equation 1). If all transported heavy ions are ordered according to mass, then the heavy ion (A>4 & Z>2) transport equation can be succinctly written as

$$\left[\frac{\partial}{\partial x} - \frac{1}{A_j}\frac{\partial}{\partial E}S_j(E) + \sigma_j(E)\right]\phi_j(x,E) = \sum_{k>j}\sigma_{k\to j}(E)\phi_k(x,E), \tag{2}$$

where $\sigma_{k\to j}(E)$ is the production cross section for interactions in which a type k particle with energy E produces a type j particle with energy E. The upper summation limit in equation 2 can vary, and OLTARIS currently uses 59 ions (See Table 2). For light particles, the equal velocity approximation is not valid and both the light projectile and the target fragments are included in the transport procedure. In this case, equation 1 is solved, and the summation is taken over all light particles: the first six particles in Table 2.

The light ion and heavy ion transport solution methodology is expressed in marching algorithms and have been analytically shown to be accurate to $O(h^2)$ where h is the step-size in units of $\frac{g}{cm^2}$.[4] Slaba et al.[54] have also controlled the energy discretization error through various modifications to the light ion transport algorithm. An extensive review of the verification and validation efforts associated with the HZETRN2005 marching algorithms can be found in Wilson et al.[5] A detailed derivation of the marching algorithms including the recent updates, can be found in Slaba et al.[54]

In the current OLTARIS implementation, two transport scenarios are used:

1. Three material layer database for interpolation currently set to aluminum, polyethylene, and tissue.
2. Multiple layer slab with coupled bi-directional neutron transport.

Item 1 generates a database of every combination of the three materials from $0.05\frac{g}{cm^2}$ for SPE and LEO and $0.1\frac{g}{cm^2}$ for GCR to $100\frac{g}{cm^2}$ with a spatial grid created to ensure spatial convergence of the marching algorithm. The slab solution allows the user to create materials and layer them so that a response function can be generated at the end of the slab and at each user defined thickness in the slab. The slab solution also allows a backward solution for neutrons.

VI. Response Functions

Once a flux or fluence spectrum over particles and energies is calculated from the Boltzmann equation, equation 1, then that flux has to be modified to represent the response wanted by the user. Currently, OLTARIS determines dose (D), dose equivalent (H), thermo-luminescence detector (TLD), Linear Energy Transfer (LET), and effective whole body dose equivalent (ED) for the interpolation transport scheme explained in Section V. Therefore, D, H, TLD, and LET are determined at each of the interpolation edit points and are interpolated over a thickness file described in Section II.B to get the values at a point inside a geometry. Each of these responses is discussed in detail below.

Table 2. HZETRN2005 Transported Isotopes

Isotope	A	Z	Isotope	A	Z	Isotope	A	Z
Neutron	1	0	H^1	1	1	H^2	2	1
H^3	3	1	He^3	3	2	He^4	4	2
Li^6	6	3	Li^7	7	3	Be^8	8	4
Be^9	9	4	B^{10}	10	5	B^{11}	11	5
C^{12}	12	6	C^{13}	13	6	N^{14}	14	7
N^{15}	15	7	O^{16}	16	8	O^{17}	17	8
F^{18}	18	9	F^{19}	19	9	Ne^{20}	20	10
Ne^{21}	21	10	Ne^{22}	22	10	Na^{23}	23	11
Mg^{24}	24	12	Mg^{25}	25	12	Mg^{26}	26	12
Al^{27}	27	13	Si^{28}	28	14	P^{29}	29	15
S^{30}	30	16	S^{31}	31	16	S^{32}	32	16
Cl^{33}	33	17	Ar^{34}	34	18	Cl^{35}	35	17
Ar^{36}	36	18	K^{37}	37	19	Ar^{38}	38	18
K^{39}	39	19	Ca^{40}	40	20	Ca^{41}	41	20
Ca^{42}	42	20	Sc^{43}	43	21	Ti^{44}	44	22
Ti^{45}	45	22	Ti^{46}	46	22	Ti^{47}	47	22
V^{48}	48	23	V^{49}	49	23	Cr^{50}	50	24
Cr^{51}	51	24	Cr^{52}	52	24	Mn^{53}	53	25
Mn^{54}	54	25	Fe^{55}	55	26	Fe^{56}	56	26
Co^{57}	57	27	Ni^{58}	58	28			

A. Dose

While the flux of particles is a detailed quantity describing the environment inside a spacecraft, it is of little use to inform the user about the damage or the risk of this particle environment to humans, material, or electronics. As a first step, the dose is calculated from the energy deposited along every particle's track as it traverses the spacecraft. Therefore, the dose is defined as:

$$D = \sum_j D_j,$$

where,

$$D_j = \int_0^\infty dE\ S_j(E)\phi_j(E) + d^\star(E)$$

with, $S_j(E)$ as the stopping power of a charged particle j at energy E in the material of interest (usually tissue or silicon) in units of $\frac{keV}{\mu m}$. If the stopping power of a charged particle does not exist, then a scaled proton stopping power can be used: $S_j(E) = \frac{Z_j^2}{A_j} S_{\text{proton}}(E)$. Of course, the stopping power of neutral particles does not exist, and the integral term is zero. Since target fragments and recoil nuclei are not transported, their dose is added by the $d^\star(E)$ function. The units of Dose are mGy.

The dose is calculated at all interpolation grid points or slab points and is called the Dose Table or Dose versus Depth Table. This table can be interpolated over a set of thickness files to obtain a dose at a point inside a vehicle and/or human.

B. Dose Equivalent

While dose gives the energy deposited by a particle in a material, it does not accurately estimate the probability of stochastic effects in humans such as cancer mortality. For the "complex mixture of high- and

low-LET radiation experienced in LEO,"[55] the National Council on Radiation Protection and Measurement (NCRP) endorses the use of dose equivalent calculated with the ICRP-60[56] quality factor, $Q_{\text{ICRP}-60}$, for this purpose.[55,57,58] As yet, the NCRP has not made a recommendation for space environments beyond LEO,[58] but NASA has adopted the approach of using dose equivalent for Constellation vehicles as well.[59] Dose Equivalent is defined as:

$$H = \sum_j H_j,$$

where,

$$H_j = \int_0^\infty dE \; Q_{\text{ICRP}-60}\left(S_j(E)\right) S_j(E)\phi_j(E) + h^\star(E).$$

The quality factor $Q_{\text{ICRP}-60}$ is defined as[56]

$$Q_{\text{ICRP}-60}\left(S_j(E)\right) = \begin{cases} 0 < S_j(E) \leq 10 & = & 1 \\ 10 < S_j(E) \leq 100 & = & 0.32S_j(E) - 2.2 \\ 100 > S_j(E) & = & \frac{300}{\sqrt{S_j(E)}} \end{cases},$$

where $S_j(E)$ is the stopping power of a charged particle j at energy E in the material, tissue, or organ of interest in units of $\frac{keV}{\mu m}$. If the stopping power of a charged particle does not exist, then a scaled proton stopping power can be used: $S_j(E) = \frac{Z_j^2}{A_j} S_{\text{proton}}(E)$. Of course, the stopping power of neutral particles does not exist and the integral term is zero. Since target fragments and recoil nuclei are not transported, their dose equivalent is added by the $h^\star(E)$ function. The units of Dose Equivalent are mSv.

The dose equivalent is calculated at all interpolation grid points or slab points and is called the Dose Equivalent Table or Dose Equivalent versus Depth Table. This table can be interpolated over a set of thickness files to obtain a dose equivalent value at a point inside a vehicle and/or human.

C. TLD-100

For dosimetry measurement purposes, one of the most widely used phosphors based instruments is the Lithium-Fluoride thermo-luminescence detector (TLD-100). These instruments are routinely flown on ISS and STS missions and were used for validation of OLTARIS. Within OLTARIS, the flux response function for the TLD-100 sensitivity to an incoming ion of charge Z and energy E is modeled by the functional fit:[60]

$$F_{\text{TLD}}(E, Z) = 0.2418 + 0.8205 * e^{-0.002*(\frac{y(Z)}{y(E)})^2},$$

where

$$y(Z) = Z\left[1 - e^{-125*(\frac{\gamma}{Z})^{\frac{2}{3}}}\right],$$

and

$$\gamma(E) = \sqrt{1 - \frac{1}{(1 + \frac{E}{932})^2}}.$$

The non-dimensional quantity $F_{\text{TLD}}(E, Z)$ then scales the appropriate flux values at a given depth, energy, and charge. Finally, the scaled fluxes are integrated over energy and summed over charge to get the TLD-100 response to the particle field.

The TLD-100 response is calculated at all interpolation grid points or slab points and is called the TLD-100 Table or TLD-100 versus Depth Table. This table can be interpolated over a set of thickness files to obtain a TLD-100 value at a point inside a vehicle and/or human.

D. Integral and Differential Linear Energy Transfer (LET)

In analyzing charged particle spectra in space due to GCR, SPE, and trapped protons, the conversion or mapping of particle energy spectra into LET distributions is a convenient guide in assessing biologically significant components of these spectra. The mapping of LET to energy is a triple valued function and can be defined only on open energy subintervals where the derivative of LET with respect to energy is not zero. OLTARIS uses a well-defined numerical procedure which allows for the generation of LET spectra on the open energy subintervals that are integrable in spite of their singular nature.[61,62] Due to the biological significance of tissue, all LET related calculations use tissue as the target material at this time. However, the numerical algorithms are identically applicable to the silicon based materials for the study of electronics and other materials for other studies. This capability will be implemented soon.

Currently, no heavy target fragments or recoils are included in the LET calculation, but they are included for the light ion (A<4) calculation.

The differential and integral LET distributions are calculated at all interpolation grid points or slab points and are called the LET Distributions or LET versus Depth Distributions. These distributions can be interpolated over a set of thickness files to obtain a differential and integral LET distribution at a point inside a vehicle and/or human.

The units of differential LET based flux are $\frac{particles}{cm^2 \frac{keV}{\mu m} day-or-event}$. The units of integral or cumulative LET based flux are $\frac{particles}{cm^2-day-or-event}$. LET has units of $\frac{keV}{\mu m}$.

E. Effective and Organ Averaged Dose Equivalent

As is recommended in NCRP-132 and NCRP-142,[55,57] effective dose equivalent is calculated by first calculating the averaged dose equivalent for the organs and tissues listed in Table 3. A weighted average of these organ or tissue dose equivalent values, as defined in equation 3, is then calculated using the NCRP-132 tissue weighting factors given in the top row of Table 3.

$$ED = \sum_{T} w_T \bar{H}_T, \tag{3}$$

where w_T are the NCRP-132 tissue weighting factors in Table 3 and $\bar{H}_T$ are the organ or tissue averaged dose equivalents as calculated by OLTARIS.

Table 3. NCRP 132 Organs and their weights

Tissue Weights	0.01	0.05	0.12	0.20
Tissue Types	Bone Surface Skin	Bladder Breast Liver Esophagus Thyroid Remainder	Bone Marrow Colon Lung Stomach	Gonads

The remainder organs are listed in NCRP-132 as: adrenals, brain, small intestine, large intestine, kidneys, muscle, pancreas, spleen, thymus, and uterus. OLTARIS also computes organ averaged dose equivalents for the following tissues (these are not included in te effective dose equivalent calculation): heart, hippocampus, lens, and salivary glands. Currently, the user can select either CAM, CAF, MAX, or FAX to compute effective dose equivalent. See reference[59] for a more detailed discussion of the methods used to analyze tissues in these human phantoms.

VII. Summary and Future Work

The OLTARIS website is a very versatile tool in the analysis of spacecraft for use with human space flight that enables the designers to meet NASA's requirements for space radiation protection throughout all stages

of vehicle design. The tools within OLTARIS are securely managed, have undergone a rigorous verification and validation process, and are presented to the user in an easy to follow format that mimics how the user wants to operate. This is achieved with modern tools, a modern understanding of how user's operate, and with many people thinking through this problem to get a solution that best fits the tools available and the user's needs and wants.

Tools are available to the materials and spacecraft design community on the OLTARIS website. A user can define their own material and transport any available space environment through it or through multiple slabs of any reasonable thickness.

OLTARIS can be easily modified to accommodate new user needs and wants. Adding new features is straight forward because of the nature of the web interface. Adding new calculations is also straight forward due to the modularity of the computational engine behind the website. The connection of the website interface to the analysis modules with the Sun Grid Engine allows external sites to be incorporated, with appropriate security issues resolved, to execute new models without giving control of those calculations to the OLTARIS team. Interface file formats are clearly defined and can be used to connect new parts with old parts to create new calculations. All of these functions are connected through use cases.

For the near future, use cases will be generated for the STS Tissue Equivalent Proportional Counter (STS-TEPC), electronic response functions either within OLTARIS or in conjunction with other sites, and new transport algorithms. The near term transport algorithm addition will be a ray-by-ray transport where the HZETRN2005 transport algorithm is executed along each ray in the spacecraft's thickness file. Each ray will have a complete slab based transport calculation performed. The results for each ray will then be integrated together to obtain the response wanted by the user.

Longer term projects include Monte Carlo solutions for slab geometries, more user control of the existing HZETRN2005 transport algorithms, new tracked particles in the HZETRN2005 marching algorithm like electrons and pions, and better and more accurate interaction cross sections to replace NUCFRG2. Of course, as this tool becomes more mature and gains users, the users will drive future improvements and priorities.

Acknowledgments

This work was supported by the Human Research Program (HRP) in the Advanced Capabilities Division (ACD) under the Exploration Systems Mission Directorate (ESMD) and performed by members of the Design Tool Project in the Space Radiation Program Element.

References

[1]NASA, "NASA Standards for Modeling and Simulation," NASA-STD-7009.

[2]Blattnig, S.R., Luckring, J.M., Morrison, J.H., Sylvester, A.J., Tripathi, R.K., and Zang, T.A., "NASA Standard for Models and Simulations: Philosophy and Requirements Overview," AIAA-2009-1010, 47th AIAA Aerospace Sciences Meeting including The New Horizons Forum and Aerospace Exposition, Orlando, Florida, Jan. 5-8, 2009.

[3]Singleterry, R.C., Wilson, J.W., Shinn, J.L., Tripathi, R.K., Thibeault, S.A., Noor, A.K., Cucinotta, F.A., Badavi, F.F., Chang, C.K., Qualls, G., Clowdsley, M.S., Kim, M.Y., Heinbockel, J.H., Norbury, J.W., Blattnig, S.R., Miller, J., Zeitlin, C., Heilbronn, L.H., "Creation and utilization of a world wide web based space radiation effects code: SIREST," Physica Medica, vol. XVII, suppl. 1, p. 90 (2001).

[4]Wilson, J. W., Townsend, L. W., Schimmerling, W., Khandelwal, G. S., Khan, F., Nealy, J. E., Cucinotta, F. A., Simonsen, L. C., Shinn, J. L., and Norbury, J. W., *Transport Methods and interactions for Space Radiations*, NASA RP-1257, 1991.

[5]Wilson, J.W., Tripathi, R.K., Mertens, C.J., Blattnig, S.R., Clowdsley, M.S., Cucinotta, F.A., Tweed, J., Heinbockel, J.H., Walker, S.A., Nealy, J.E., "Verification and Validation: High Charge and Energy (HZE) Transport Codes and Future Development," NASA Technical Paper 213784, 2005.

[6]Wilson, J.W., Tripathi, R., Cucinotta, F., Shinn, J., Badavi, F., Chun, S., Norbury, J.W., Zeitlin, C.J., Heilbronn, L., Miller, J., "NUCFRG2: An evaluation of the semiempirical nuclear fragmentation database," NASA Technical Paper 3533, 1995.

[7]Wilson, J.W., Townsend, L.W., Badavi, F.F., "A semi-empirical nuclear fragmentation model," Nuclear Instruments and Methods in Physics Research B, Vol. 18, pp. 225-231, 1987.

[8]Wilson, J.W., Shinn, J.L., Townsend, L.W., Tripathi, R.K., Badavi, F.F., Chun, S.Y., "NUCFRG2: a semi-empirical nuclear fragmentation model," Nuclear Instruments and Methods in Physics Research B, Vol. 18, pp. 95-102, 1994.

[9]Wilson, J.W., Townsend, L.W., Nealy, J.E., Chun, S.Y., Hong, B.S., Buck, W.W., Lamkin, S.L., Ganapol, B.D., Khan, F., Cucinotta, F.A., "BRYNTRN: A Baryon Transport Model," NASA Technical Paper 2887, 1989.

[10]http://rubyonrails.org/

[11]http://www.mysql.com/

[12]http://httpd.apache.org/

[13]http://gridengine.sunsource.net/

[14]Yucker, W.R., Huston, S.L., "The Computerized Anatomical Female," Final Report MDC-6107, McDonnell Douglas Company, 1990.

[15]Yucker, W.R., Reck, R.J., "Computerized Anatomical Female Body Self-Shielding Distributions," Report, MDC 92H0749, McDonnell Douglas Company, 1992.

[16]Billings, M.P., Yucker, W.R., "The Computerized Anatomical Man (CAM) Model," Summary Final Report, MDC-G4655, McDonnell Douglas Company, 1973.

[17]Kramer, R., Vieira, J.W., Khoury, H.J., Lima, F.R.A., Fuelle, D., "All about MAX: A Male Adult Voxel Phantom for Monte Carlo Calculations in Radiation Protection Dosimetry," Physics in Medicine and Biology, Vol. 48, pp. 1239-1262, 2003.

[18]Kramer, R., Vieira, J.W., Khoury, H.J., Lima, F.R.A., Loureiro, E.C.M., Lima, V.J.M., Hoff, G., "All about FAX: A Female Adult Voxel Phantom for Monte Carlo Calculations in Radiation Protection Dosimetry," Physics in Medicine and Biology, Vol. 49, pp. 5203-5216, 2004.

[19]http://www.pmddtc.state.gov/regulations_laws/itar_official.html

[20]Fasso, A., Ferrari, A., Ranft, J., Sala, P.R., "FLUKA: a multi-particle transport code," CERN-2005-10, INFN/TC 05/11, SLAC-R-773, 2005.

[21]Waters, L.S., McKinney, G.W., Durkee, J.W., Fensin, M.L., Hendricks, J.S., James, M.R., Johns, R.C., & Pelowitz, D.B., "The MCNPX Monte Carlo radiation transport code," American Institute of Physics Conference Proceedings, Vol. 896, p. 81, 2007.

[22]GEANT4, Users's Documents, Physics Reference Manual, http://wwwinfo.cern.ch/asd/geant4/G4UsersDocuments/UsersGuides/PhysicsReferenceManual, 1998.

[23]Niita, K., Sato, T., Nakashima, H., Iwase, H., Nose, H., Sihver, L., "PHITS: A particle and heavy ion transport code system," Radiation Measurements, Vol. 41, pp. 1080-1090, 2006.

[24]Townsend, L.W., Miller, T.M., Gabriel, T.A., "HETC Radiation Transport Code Development for Cosmic Ray Shielding Applications in Space," Radiation Protection Dosimetry, Vol. 115, pp. 135-139, 2005.

[25]Mokhov, N.V., Striganov, S.I., Van Ginneken A., Mashnik, S.G., Sierk, A.J., Ranft, R., "MARS Code Developments," Los Alamos National Laboratory Report LA-UR-98-5716, 1998.

[26]Hufner, J., Schafer, K., Schurmann, B., "Heavy fragments produced in proton-nucleus and nucleus-nucleus collisions at relativistic energies," Physical Review C, Vol. 12, pp. 1888-1898, 1975.

[27]Norman, R., Blattnig, S., Norbury, J., "Nuclear fragmentation model evaluation," Meeting of the Southeastern section of the American Physical Society, Raleigh, North Carolina, October 2008.

[28]Wilson, J.W., Townsend, L.W., Buck, W.W., Chun, S.Y., Hong, B.S., Lamkin, S.L., "Nucleon-Nucleus Interaction Data Base: Total Nuclear and Absorption Cross Sections," NASA Technical Memorandum 4053, 1988.

[29]Cucinotta, F.A., Townsend, L.W., Wilson, J.W., "Description of alpha-nucleus interaction cross sections for cosmic ray shielding studies," NASA Technical Paper 3285, 1993.

[30]Cucinotta F.A., "Calculations of Cosmic-Ray Helium Transport in Shielding Materials," NASA Technical Paper 3354, 1993.

[31]Cucinotta, F.A., Townsend, L.W., Wilson, J.W., Shinn, J.L., Badhwar, G.D., Dubey, R.R., "Light ion components of the galactic cosmic rays: nuclear interactions and transport theory," Advances in Space Research, Vol. 17, pp. 77-86, 1996.

[32]Tripathi, R.K., Wilson, J.W., Cucinotta, F.A., "New Parameterization of Neutron Absorption Cross Sections," NASA Technical Paper 3354, 1997.

[33]Tripathi, R.K., Cucinotta, F.A., Wilson, J.W., "Universal Parameterization of Absorption Cross Sections," NASA Technical Paper 209726, 1999.

[34]Norbury, J.W., "Nucleon-Nucleon Total Cross Section," NASA Technical Paper 215116, 2008.

[35]Tai, H., Bichsel, H., Wilson, J.W., Shinn, J.L., Cucinotta, F.A., Badavi, F.F., "Comparison of stopping Power and Range Databases for Radiation Transport Study," NASA Technical Paper 3644, 1997.

[36]O'Neill, P.M., *et al.*, "Badhwar-O'Neill Galactic Cosmic Ray Model Update Based on Advanced Composition Explorer (ACE) Energy Spectra from 1977 to Present," Advances in Space Research, Vol. 37, pp. 1727-1733, 2006.

[37]NASA, Constellation Program Design Specification for Natural Environments (DSNE), CxP 70023, Rev A, Change 001, Nov 7, 2008.

[38]Webber, W.R., "An Evaluation of the Radiation Hazard due to Solar-Particle Events," D2-90469 Aero-Space Div., Boeing Co., 1963.

[39]King, J.H., "Solar proton fluences for 1977 - 1983 space missions," Journal of Spacecraft and Rockets, Vol. 11, No. 6, pp. 401-408, 1974.

[40]Sauer, H.H., *et al.*, "Summary Data for the Solar Energetic Particle Events of August Through December 1989," Space Environment Laboratory, National Oceanic and Atmospheric Administration, 1990.

[41]Townsend, L.W., Zapp, E.N., Stephens, D.L., Hoff, J.L., "Carrington Flare of 1859 as a Prototypical Worst-Case Solar Energetic Particle Event," IEEE Transactions on Nuclear Science, Vol. 50, No. 6, Dec. 2003.

[42]Sawyer, D.M., *et al.*, "AP-8 Trapped Proton Environments for Solar Maximum and Solar Minimum," NSSDC/WDC-A-R&S, 76-06, 1976.

[43]Vette, J.I., "The NASA/National Space Science Data Center Trapped Radiation Environmental Model Program (1964-1991)," NSSDC/WDC-A-R&S 91-29, 1991.

[44]Foelsche, T., *et al.*, "Measured and Calculated Neutron Spectra and Dose Equivalent Rates at High Altitudes," Relevance to SST Operations and Space Research, NASA TN D-7715, 1974.

[45]Wilson, J.W., *et al.*, "Cosmic Ray Neutron Albedo Dose in Low Earth Orbit," Health Physics, Vol. 57, pp. 665-668, 1989.

[46]Wilson, J.W., *et al.*, "Preliminary Analysis of the Implications of Natural Radiations on Geostationary Operations," NASA TN D-8290, 1976.

[47]De Angelis, G., *et al.*, "A new Dynamical Atmospheric Ionizing Radiation (AIR) Model for Epidemiological Studies," Advances in Space Research, Vol. 32(1), pp. 17-26, 2003.

[48]Clem, J.M., *et al.*, "Preliminary Validation of Computational Procedures for a new Atmospheric Ionizing Radiation (AIR) Model," Advances in Space Research, 32(1), 27-33, 2003.

[49]Wilson, J.W., *et al.*, "International Space Station: A Test bed for Experimental and Computational Dosimetry," Advances in Space Research, Vol. 37, pp. 1656-1663, 2006.

[50]Jensen, D.C., *et al.*, "An Interim Geomagnetic Field," Journal of Geophysical Research, No. 67, pp. 3568-3569, 1962.

[51]Cain, J.C., *et al.*, "A Proposed Model for the International Geomagnetic Reference Field-1965," Journal of Geomagnetism and Geoelectricity, No. 19, pp. 335-355, 1967.

[52]Wilson, J.W., Badavi, F.F., "Methods of Galactic Heavy Ion Transport," Radiation Research, Vol. 108, pp. 231-237, 1986.

[53]Cucinotta, F.A., "Calculations of Cosmic-Ray Helium Transport in Shielding Materials," NASA Technical Paper 3354, 1993.

[54]Slaba, T.C., Blattnig, S.R., Clowdsley, M.S., Walker, S.A., Badavi, F.F., "An Improved Neutron Transport Algorithm for HZETRN2005," Advances in Space Research, submitted, 2008.

[55]National Council on Radiation Protection and Measurements (NCRP), "Operational Radiation Safety Program for Astronauts in Low-Earth Orbit: A Basic Framework," NCRP Report 142, 2002.

[56]International Commission on Radiological Protection (ICRP), "The 1990 Recommendations of the International Commission on Radiological Protection," ICRP Publication 60, Elsevier, New York, 1993.

[57]National Council on Radiation Protection and Measurements (NCRP), "Radiation Protection Guidance for Activities in Low-Earth Orbit," NCRP Report 132, 2000.

[58]National Council on Radiation Protection and Measurements (NCRP), "Information needed to make radiation protection recommendations for space missions beyond low Earth orbit," NCRP Report 153, 2006.

[59]Slaba, T.C., Qualls, G.D., Clowdsley, M.S., Blattnig, S.R., Simonsen, L.C., Walke, S.A., Singleterry, R.C., "Analysis of Mass Averaged Tissue Doses in CAM, CAF, MAX, and FAX", NASA-TP-2009-215562, 2009.

[60]Wilson, J.W., Tripathi, R.K., Badavi, F.F., Cucinotta, F.A., "Standardized Radiation Shield Design Method: 2005 HZETRN," International Conference on Environmental Systems (ICES), Norfolk, VA, No. 2006-01-2109, 2006.

[61]Badavi, F.F., Wilson, J.W., Hunter, A., "Numerical study of the generation of linear energy transfer spectra for space radiation applications," NASA-TP-2005-213941, 2005.

[62]Badavi, F.F., Stewart-Sloan, C.R., Adams, D.O., and Wilson, J.W., "Radiation Protection Effectiveness of Polymeric Based Shielding Materials at Low Earth Orbit," SAMPE, No. 2008-L002, May 2008.